Colloids and Surfaces B: Biointerfaces 143 (2016) 490–498

Contents lists available at ScienceDirect

Colloids and Surfaces B: Biointerfaces

journal homepage: www.elsevier.com/locate/colsurfb

# Antibacterial activity of graphene supported FeAg bimetallic nanocomposites

Ayyaz Ahmad[a], Abdul Sattar qureshi[b], Li Li[a], Jie Bao[b], Xin Jia[c], Yisheng Xu[a,**], Xuhong Guo[a,c,**]

[a] State Key Laboratory of Chemical Engineering, East China University of Science and Technology, Shanghai 200237, China
[b] State key Laboratory of Bioreactor Engineering, East China University of Science and Technology, Shanghai 200237, China
[c] Department of Chemical Engineering, Shihezi University, Xinjiang 832000, China

ARTICLE INFO

*Article history:*
Received 4 September 2015
Received in revised form 14 March 2016
Accepted 22 March 2016
Available online 23 March 2016

*Keywords:*
FeAg bimetallic
Graphene
Antibacterial activity
Reactive oxygen species
GSH oxidation

ABSTRACT

We report the simple one pot synthesis of iron-silver (FeAg) bimetallic nanoparticles with different compositions on graphene support. The nanoparticles are well dispersed on the graphene sheet as revealed by the TEM, XRD, and Raman spectra. The antibacterial activity of graphene-FeAg nanocomposite (NC) towards *Bacillus subtilis*, *Escherichia coli*, and *Staphylococcus aureus* was investigated by colony counting method. Graphene-FeAg NC demonstrates excellent antibacterial activity as compared to FeAg bimetallic without graphene. To understand the antibacterial mechanism of the NC, oxidative stress caused by reactive oxygen species (ROS) and the glutathione (GSH) oxidation were investigated in the system. It has been observed that ROS production and GSH oxidation are concentration dependent while the increase in silver content up to 50% generally enhances the ROS production while ROS decreases on further increase in silver content. Graphene loaded FeAg NC demonstrates higher GSH oxidation capacity than bare FeAg bimetallic nanocomposite. The mechanism study suggests that the antibacterial activity is probably due to membrane and oxidative stress produced by the nanocomposites. The possible antibacterial pathway mainly includes the non-ROS oxidative stress (GSH oxidation) while ROS play minor role.



## 1. Introduction

Contamination especially in the environment and generally in drinking water is one of the most critical issues in the world [1]. Various pollutants such as heavy metals, organic compounds, and microorganism especially bacteria have become a severe threat for human lives [2–4]. The bacterial growth rate is very prompt under favorable conditions and causes lots of diseases [5]. On the other hand, due to extensive use of antibiotics, these bacteria can develop the tolerance against the antibacterial action. Moreover, bacteria can be one type of contamination where the hygienic conditions are required due to their growth on the surface [6]. These problems become more severe when diseases caused by pathogens are engaged in the food industry [7]. Therefore the development of new materials has become essential to suppress bacterial activity. The ideal antibacterial material should be non-toxic, cheap, environmentally friendly, and display excellent antibacterial activity [8,9].

Iron is one of the most frequently used metal for treatment of contaminants present in water [2]. It is the fourth most abundant element after oxygen, silicon and aluminum present in the earth crust [10]. Iron NP has been used from the treatment of various harmful pollutants such as chlorinated compounds in wastewater [11,12]. Low cost, non-toxic, and high reactivity make iron as a first choice for the researcher [13]. However, little is known for the mechanism in antimicrobial applications. *Bacillus subtilis* and *Escherichia coli* are the most studied bacteria using Fe NPs [14–16]. Lee et al. concluded that better antibacterial activity of *E. coli* was achieved using Fe NPs [17], but the rapid oxidative corrosion of Fe NPs has limited its application. It was proven that Fe NPs could be more efficient and effective [18]. Alternatively, silver related NPs were also used as antibacterial agents [19–21]. $Ag^{+}$ ions interact with the bacterial cells and alter the main function causing the cell death [22]. As reported, silver NPs anchored on graphene oxide sheets manifest excellent antibacterial activity for *P. aeruginosa* [7]. Bimetallic Fe-Ag NPs has shown significant antimicrobial activity while Fe alone did not show any bactericidal effect on the microbial growth perhaps due to corrosion [23].

** Corresponding authors at: State Key Laboratory of Chemical Engineering, East China University of Science and Technology, Shanghai 200237, China.
*E-mail addresses:* yshxu@ecust.edu.cn (Y. Xu), guoxuhong@ecust.edu.cn, guoxuhong@hotmail.com (X. Guo).

http://dx.doi.org/10.1016/j.colsurfb.2016.03.065
0927-7765/

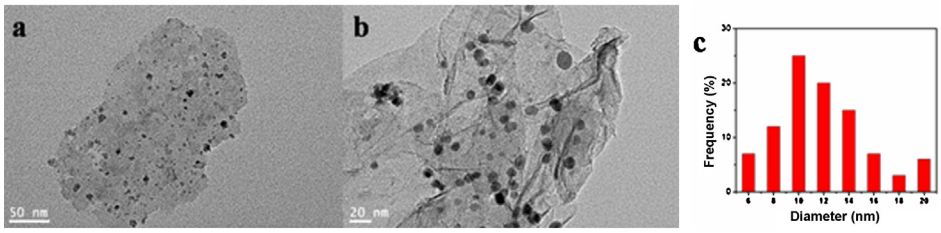


**Fig. 1.** TEM (a and b) and size distribution (c) of $Fe_7Ag_1$ decorated on the graphene sheet.

Graphene with 2-D structure receives lot of attentions due to its versatile physiochemical properties such as large surface area, high mechanical, and high electrical stability [24]. It has been widely applied with other materials in the preparation of NC to enhance their properties [25,26]. Graphene not only enhances the activity but also provides a stable support for the inorganic materials [27–29]. These graphene-inorganic NC as well as graphene itself shows toxicity towards pathogens. Quite a few researches are being focused on the antibacterial activity of graphene and its related derivatives [30,31].

In this work, Fe-Ag bimetallic NPs with different compositions were synthesized *in situ* using $NaBH_4$ as a reducing agent on graphene oxide. The NC was characterized by XRD, TEM, EDS, and Raman spectroscopy. To the best of our knowledge, this is the first report on the combined effect of these materials in the antibacterial activity of *B. subtilis*, *S. aureus*, and *E. coli*. Our main aim is to enhance the antibacterial activity of iron based NC, because better antibacterial effect by iron seems more necessary for more practical applications. Iron based antibacterial materials would be cost effective. A much more effective antibacterial material is developed based on bimetallic NC attached graphene in contrast to simple bimetallic NPs previously reported for high antibacterial activity. The effect of graphene-FeAg concentration on these three different bacteria was investigated. To get the better understanding in terms of antibacterial mechanism, the oxidative stress caused by graphene-bimetallic nanocomposite was systematically studied. Superoxide ($^{\bullet}O_2^-$) radicals induced by reactive oxygen species (ROS) generation was quantified by using the *p*-nitroblue tetrazolium chloride method. In-vitro glutathione oxidation method was performed to examine the non-ROS oxidative stress effect.

## 2. Experimental

### 2.1. Materials

Natural graphite obtained from Qingdao NanshuRuiying Graphite Co. Ltd., China. Ferrous sulfate ($FeSO_4{\cdot}6H_2O$, 99.5%), sodium chloride (NaCl, 99.5%), sodium nitrate, $H_2SO_4$, $KMnO_4$, and $H_2O_2$ were obtained from Shanghai Jingchun Reagent Ltd. Co. (Shanghai, China). Silver nitrate ($AgNO_3$) was purchased from Sinopharm chemical research Co. The water used in the experiment was purified with a Millipore Milli-Q system.

### 2.2. Synthesis of graphene oxide (GO)

GO was synthesized from natural graphite flakes using the modified Hummers method [32,33]. In the given process, graphite (2.0 g) and $NaNO_3$ (1.0 g) were added to 50 mL of concentrated $H_2SO_4$ (98%), and the mixture was mechanically stirred in an ice bath for 2 h. $KMnO_4$ (7.3 g) was slowly added to the mixture, then 7 mL of $H_2O_2$ and 150 mL of deionized water were added respectively. Thus the colour of the mixture changed from brown into bright yellow. The mixture was filtered and washed several times with 3% HCl solution and de-ionized water. GO was vacuum-dried at 40 °C for 24 h and obtained as brown solid. The obtained product was dispersed in 500 mL water through ultra-sonication. In the end, solid form of GO was obtained by centrifugation and vacuum drying at 40 °C for 24 h.

### 2.3. Synthesis of graphene-FeAg nanocomposite

In the typical reaction, 0.5 mg/mL GO (50 mL) dispersion was prepared through ultra-sonication for one hour. Then, we added 20 mL mixed salt solution with different mole concentration of iron/silver salts (Fe 10 mM/Ag 0 mM, Fe 8.75 mM/Ag 1.25 mM, Fe 7.5 mM/Ag 2.5 mM, and Fe 5 mM/Ag 5 mM) in GO dispersion and continued ultra-sonication for one hour then half an hour through magnetic stirrer. After mixing, 1.0 g of $NaBH_4$ dissolved in 40 mL of water was added to the mixture dropwise at 75–80 °C for two hours. The color of mixture turned into black. Then the mixture was cooled down at room temperature. The black solid was separated from the mixture through filtration by washing with water and ethanol respectively. The obtained product was dried at the 50 °C under the vacuum for 24 h before the characterization or further use. For the synthesis of graphene and FeAg bimetallic without graphene, we followed the same procedure except for adding the salt or graphene, respectively.

### 2.4. Characterization

The high transmission electron microscopy (TEM) was performed using a JEOL-2100 electron microscope operating at 200 kV. X-ray diffraction (XRD) was carried out on a Bruker D8 Advance X-ray diffractometer with a scan rate of 6°/min. Raman spectra of the samples were recorded by Renishaw inVia Reflex Raman spectroscopy.

### 2.5. Antibacterial activity

Antibacterial activity of *B. subtilis W800, E. coli BL21*, and *Staphylococcus aureus* was investigated by G-FeAg nanocomposite. Before the start of any antibacterial activity, all the glassware and samples were autoclaved at 121 °C for 20 min. All the bacteria were cultured in LB medium at 37 °C for 12 h 1.0 mL of saline solution washed bacterial cells were added in the saline solution for maintaining the $\sim 10^6$ colony forming unit (CFU/mL). After that, 1–200 μg/mL amount of catalyst (from aqueous suspension of 5 g/L of catalyst) was added in the saline solution and incubated at 37 °C in shaking incubator for two hours. After 2 h, 100 μL of serially diluted bacterial suspension was spread on the LB agar plates and incubated at 37 °C for 24 h. Cell viabilities were counted on plates after 24 h. The antibacterial activity was also verified by recording the growth OD at 600 nm to compare with the results from CFU experiments (not shown).

### 2.6. Detection of superoxide radical specie ($^{\bullet}O_2^-$) and thiol oxidation and quantification

To investigate the role of reactive oxygen species in the antibacterial activity, the generation of ROS was evaluated through measuring the absorption of *p*-nitroblue tetrazolium salt ($NBT^{2+}$). The production of ROS was detected by adding $NBT^{2+}$ to samples before incubation as it selectively reacts with $^{\bullet}O_2^-$ to form a formazan product. The decomposition of NBT was monitored at wavelength 259 nm by UV–vis spectrometer [34]. The details are given in the Supporting information.

The concentration of thiols in GSH was quantified by the Ellman's assay using the method describes in the previous studies [30]. The dispersion of G-$Fe_7Ag_1$ with different concentrations (225 μL at 10 μg/mL, 20 μg/mL, 50 μg/mL, 100 μg/mL or 200 μg/mL) and 100 μg/mL of other nanocomposites (Fe, $Fe_7Ag_1$, $Fe_3Ag_1$, $Fe_1Ag_1$, graphene, G-Fe, G-$Fe_7Ag_1$, G-$Fe_3Ag_1$, G-$Fe_1Ag_1$) in 50 mM bicarbonate buffer (pH 8.6) was added into 225 μL of GSH (0.8 mM in the bicarbonate buffer) to start the oxidation. The vials were covered with alumina foil to avoid illumination, and then placed in a rotary shaker with a speed of 150 rpm at room temperature for incubation of 2 h. After the oxidation reaction, 785 μL of 0.05 M Tris–HCl and 15 μL of DNTB (Ellman's reagent, 5,5′-dithio-bis-(2-nitrobenzoic acid), J&K chemicals) were added into the mixtures to yield a yellow product. The mixtures were filtered through a 0.20 mm surfactant-free cellulose acetate membrane to remove the catalysts present in the mixture. A 0.5 mL aliquot of solutions from each sample was then placed and their absorbance at 412 nm was measured on a UV–vis spectrophotometer. All tests were prepared in triplicate. GSH solution without catalyst was used as a negative control. GSH (0.4 mM) oxidization by $H_2O_2$ (1 mM) was used as a positive control. The loss of GSH was calculated by the given formula: loss of GSH% = (absorbance of negative control − absorbance of sample)/absorbance of negative control × 100.

## 3. Results and discussion

### 3.1. Characterizations of graphene-Fe-Ag nanocomposite

In the synthesis of Fe-Ag bimetallic on graphene, mixture of both precursors was added into GO dispersion. The reduction of both ions was realized by adding $NaBH_4$ dropwisely into the solution at 80 °C. The morphology of bimetallic NPs was examined by TEM as shown in Fig. 1. Results show that NPs are in the range of ~10 nm in diameter. The NPs were dispersed well on the graphene sheet. Graphene oxide has various functional groups and these functional groups can provide nucleation sites for the growth of NPs on graphene sheet.

XRD pattern of GO indicates its peaks at 2θ = 11.1° and 42.1° which are the characteristics peaks (Fig. S1a). Fig. 2 shows the XRD data of Fe and different composition of Fe-Ag NPs attached on the graphene sheet. The peak observed for G-Fe at around 2θ = 45° is the characteristic peak of Fe NPs. In the case of bimetallic graphene, Ag and Fe peaks overlap at 45° which confirms the presence of bimetallic NPs on the graphene, while other peaks at 38.3°, 64.7°, and 77.3° are the characteristics peaks of Ag NPs [35]. In contrast, no peak was observed for graphene. The graphene diffraction peaks disappear because NPs attached on the sheet might prevent the restacking of graphene sheet [36]. ICP results further confirm the presence of Ag and Fe in the sample and the final ratio of the Fe/Ag is very close to the feeding ratio of Fe/Ag as shown in Table S1. The above results suggest that bimetallic Fe-Ag were successfully prepared on the graphene sheets.

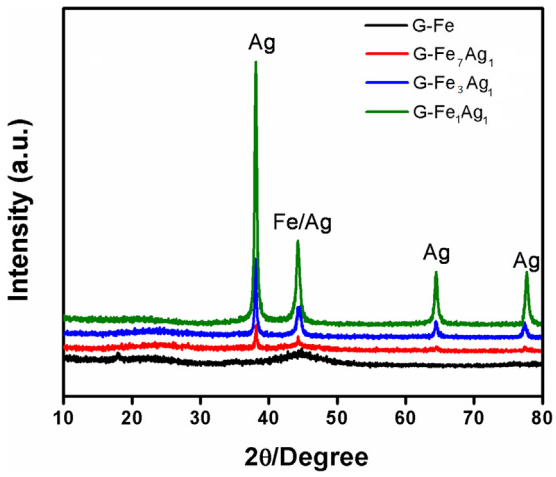


**Fig. 2.** XRD results of G-Fe and different composition of G-Fe-Ag.

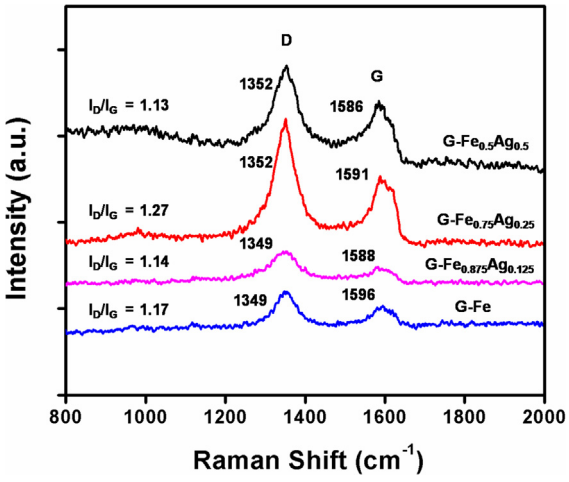


**Fig. 3.** Raman spectra of GFe, G$Fe_7Ag_1$, G$Fe_3Ag_1$, and G$Fe_1Ag_1$.

EDS mapping was also used to confirm the presence of Fe, Ag, carbon, and oxygen in NPs. Fig. S2 in Supporting information clearly indicates that large amounts of C, O, Fe, and Ag were incorporated. *In-situ* reduction of FeAg bimetallic on graphene was characterized by Raman spectroscopy, and the results are shown in Fig. 3 as compared with the Raman profile of GO shown in Fig. S1b. The spectrum of GO in Fig. S1b shows two prominent peaks at 1344 $cm^{-1}$ and 1596 $cm^{-1}$ ascribed to the D and G bands of carbon related materials respectively. Generally, the D band is associated with the breathing mode of k-point phonons of $A_{1g}$ symmetry, while the G band is related to the $E_{2g}$ phonons of $sp^2$ carbon atoms [37]. All four nanocomposites (GFe, G$Fe_7Ag_1$, G$Fe_3Ag_1$, and G$Fe_1Ag_1$) also display the D and G peaks as observed in Fig. 3. The intensity ratio of D and G band ($I_D/I_G$) can be used to investigate the removal of oxygenated groups present in the GO. In the reduction process, $sp^2$ carbon network is restored leading to an increase of $I_D/I_G$ [37,38]. It was observed that all four nanocomposite showed higher $I_D/I_G$ value (1.17, 1.14, 1.27 and 1.13) than that (1.01) of GO, indicating the successful reduction of GO. Different molar composition of Fe and Ag were synthesized and analyzed by inductively coupled plasmaatomic emission spectroscopy (ICP-AES) (see Table S1 in Supporting information).

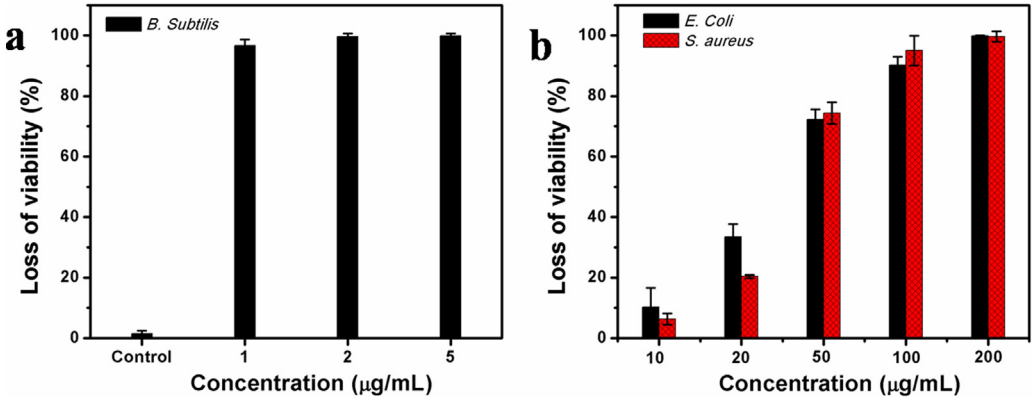


**Fig. 4.** Effect of different concentration of (G-$Fe_7Ag_1$) nanocomposite on the antibacterial activity of (a) *B. subtilis*, (1, 2, and 5 μg/mL) and (b) *E. coli* and *S. aureus* (10, 20, 50, 100, and 200 μg/mL). In control experiment, bacteria are grown without any nanocomposite.

### 3.2. Antibacterial activity of graphene-Fe-Ag nanocompsoite

Inactivation of gram positive and gram negative bacteria were investigated while using bimetallic anchored on the graphene sheets. *E. coli* and *S. aureus* are gram negative and gram positive bacteria respectively. We have selected these types of bacteria to study the effect of our mateial. While in the case of *B. subtilis*, it has shown much resistance. We want to study the effectiveness of our nanocomposite on *B. subtilis* cell death. Bimetallic NPs without graphene were used as a control. G-$Fe_7Ag_1$ was chosen to determine the effect of different concentration of G-Fe-Ag nanocomposite. Three bacteria (*B. subtilis*, *E. coli*, and *S. aureus*) were chosen for the antibacterial tests. Concentration dependent antibacterial activity of these bacteria was investigated by varying the concentration ranging from 1 to 200 μg/mL with two hour incubation.

Fig. 4 shows the effect of different concentrations of G-$Fe_7Ag_1$ on the bacterial strains. It is interesting that complete inhibition of *B. subtilis* can be achieved with a very low concentration of nanocomposite. We have tested the same concentration of nanocomposites for the *B. subtilis* as we used for other two bacteria but at that concentration we have found the same results (approximately all cells were dead). So we decreased the concentration from 10 to 200 mg/L to 1–5 mg/L where we got some comparable results. We have tested 1 μg/mL, 2 μg/mL, and 5 μg/mL of G-$Fe_7Ag_1$ for *B. subtilis* as shown in Fig. S3. Viability of the cells decreases with the concentration of catalyst, and the viability loses completely 99.6 ± 1% at 2 μg/mL (Fig. 4a).

The effects of G-$Fe_7Ag_1$ on *E. coli* and *S. aureus* were also studied in Fig. 4b which shows the increasing loss of cells viability with catalyst concentration (see Figs. S4 and 5 in Supporting information). 90.23 ± 2.75% and 95.1 ± 4.9% cell viability are lost for *E. coli* and *S. aureus* respectively when 100 μg/mL of catalyst was added. In the case of *S. aureus*, maximum antibacterial activity of G-$Fe_7Ag_1$ is observed using 100 μg/mL while nearly complete effect 98.4 ± 0.75% and 99.6 ± 1.75% was observed when 200 μg/mL was used.

We have also used 50 ug/ml concentrations of nanocomposite to check the effect of silver content for the antibacterial activity of *E. Coli* as shown in Fig. S6 in Supporting information. There is marginal increase in antibacterial activity from 53.1% to 72.1% when $GFe_7Ag_1$ instead of GFe was used. However, the increase of the activity becomes less dramatic as the silver contents (molar ratio) were increased from 0.125 to 0.5. Apparently, $GFe_7Ag_1$ would be cost effective composition due to the less content of expensive silver.

Furthermore, the effects of different compositions of bimetallic anchored graphene nanocomposite were studied. In order to examine the contribution of graphene in the metallic nanocomposite to the antibacterial performance, the effects of same composition of Fe or FeAg bimetallic without graphene were also investigated. In Fig. 5, it is obvious that bimetallic NPs loaded graphene shows excellent antibacterial activity as compared to bare bimetal-

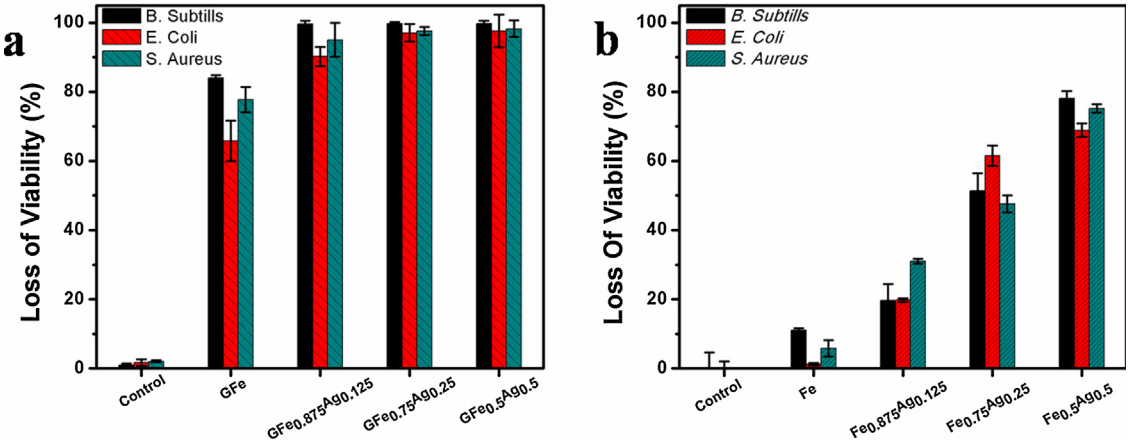


**Fig. 5.** Antibacterial activities of *B. subtilis*, *E. coli*, and *S. aureus* using (a) G-Fe, G-$Fe_7Ag_1$, G-$Fe_3Ag_1$, and G-$Fe_1Ag_1$, (b) Fe, $Fe_7Ag_1$, $Fe_3Ag_1$, and $Fe_1Ag_1$ [In control experiments of (a) and (b), growth of bacteria was observed without adding any nanocomposite or bimetallic catalyst. Concentration of different graphene-FeAg nanocomposite or bimetallic FeAg used for (*B. subtilis*, 2 μg/mL) or for *E. coli* and *S. aureus*, (100 μg/mL)].

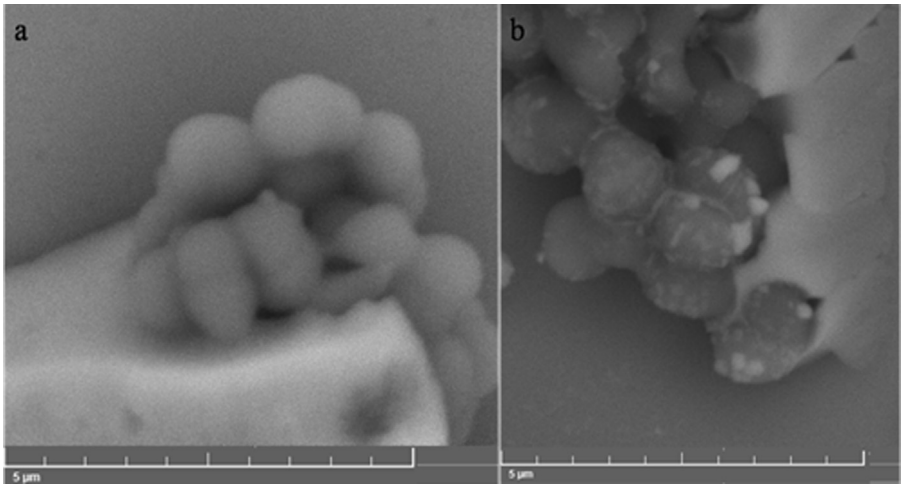


**Fig. 6.** SEM images of *S. aurues* (a) control, (b) after two hour incubation with nanocomposites.

lic NPs. When graphene was used as the substrate for metal immobilization, better activities of the metal nanocomposites with graphene were found than the corresponding metallic or bimetallic nanocomposites without graphene. Increasing the Ag content showed increasing antibacterial activities while this was not completely true in the case with bimetallic NPs loaded graphene. Here we want to demonstrate that small amount of Ag content with graphene loaded bimetallic NPs has shown significant enhancement of antibacterial activity (>90%) while increasing the Ag content did not show bigger difference. It probably reaches the limit of antibacterial effect in the current bimetallic system. In our previous work, we have done XRD of bare Fe and Fe-rGO. It was confirmed that oxide layer was formed at 18° in case of bare nZVI while this peak was not observed in case of nZVI-rGO [39]. It might conclude that Graphene not only prevents the Fe NPs from oxidation but also enhances the antibacterial activity to some extend since graphene also acts as antimicrobial agent, reported in previous studies [30,31]. Fe NPs alone show negligible activity $11 \pm 0.8\%$, $1.3 \pm 0.5\%$, and $5.8 \pm 2.4\%$ towards *B. subtilis*, *E. coli*, and *S. aureus* respectively which might be due to the formation of oxide film on the surface of the particles [23]. In the bare bimetallic NPs case, antibacterial effect increases as the mole fraction of silver is increased to $19.6 + 4.7\%$, $51.4 \pm 5.02$, $78.15 \pm 2.12$ for example in case of *B. subtilis*. However, bimetallic NPs without the graphene have shown less toxicity overall in contrast to the cases with graphene. This probably happens due to the aggregation of NPs without any support [27]. Fig. 6 shows the *S. Aureus* interaction with nanocomposites through SEM. It has observed from the SEM figure that in the control, outer surface of the bacteria is very smooth while after interaction with nanocomposite the surface become rough. We can conclude from the figure that this roughness in the surface may cause the membrane disruption in the bacterial cells.

To understand the effects of graphene or its contribution towards the antibacterial activity of these bacteria, toxicity of graphene itself on the bacteria was also studied. The result shows in Fig. S7 indicates that graphene has slight effect on the antibacterial activity of *E. coli* but it has negligible effect on the *B. subtilis*. It might be because *E. coli* is gram negative bacteria while others are gram positive bacteria. From these results, it might be concluded that *B. subtilis* inactivity using nanocomposite is attributed due to the bimetallic NPs decorated on the graphene. However, in case of *E. coli*, graphene might contribute some toxicity effects. Our nanocomposites have shown somehow better results as compare to other iron related antibacterial agents as shown in Table 1.

### 3.3. Oxidative stress studies

Oxidative stress plays vital role in the antibacterial activity as described in previous studies on the cytotoxicity of the materials [30,42,43]. Oxidative stress caused by cytotoxicity related materials was checked from two different ways. One is reactive oxygen species (ROS) and another is ROS independent oxidative stress.

In order to better understand the mechanism related to toxicity caused by graphene-bimetallic nanocomposite, ROS and non-ROS paths were investigated. To figure out the antibacterial activity through ROS, $NBT^{2+}$ was used to measure the possibility of ROS ($^{\bullet}OH$ and $^{\bullet}O_2^-$) produced in the system due to the nanocomposite. As shown in Fig. 7, $^{\bullet}O_2^-$ was detected as reflected by the degradation of $NBT^{2+}$. Fig. 7a and b show the degradation of $NBT^{2+}$ increases as the concentration of G-$Fe_7Ag_1$ increases indicating an increase of ROS amount. In case of different graphene based nanocomposites, ROS production increases to $1.007 \pm 0.131$, $0.791 \pm 0.015$ as the amount of silver content increases in the nanocomposite upto 25%, even though ROS slightly decreases to $1.01 \pm 0.141$ when 50% silver content was used.

Similar effect is observed in case of FeAg bimetallic without graphene. From the results, it is apparent that ROS production increases as graphene is used as the metal support. ROS is not only related to Fe but it can be influenced by Ag. Secondly, ROS generation can be enhanced when some metals are attached with the iron. Such results are consistent with the findings in the literature that radicals are produced in the iron based aqueous systems [44]. Therefore, ROS generated by the nanocomposite may play an important role for some extend in the antibacterial activity. The identification and role of different possible ROS for the nanocomposite should be carefully examined in further studies.

To examine the oxidative stress caused by ROS-independent path, *in vitro* GSH oxidation was performed since this path is widely used in the graphene related materials as described above [45]. GSH is a tripeptide having thiol groups and is an antioxidant presents in the bacteria at a concentration ranging from 0.1 to 10 mM. GSH can be converted to glutathione by oxidizing thiol groups (—SH) into disulfide bond (—S—S—) [43]. Ellman's assay was employed to investigate the oxidation of GSH by using different concentrations of $GFe_7Ag_1$ and other Fe-Ag bimetallic with or without graphene as shown in Figs. 8 and 9 [46]. Buffer solution (50 mM, pH = 8.6) and $H_2O_2$ (1 mM) were used as a negative control and a positive control for the GSH oxidation respectively.

**Table 1**
Comparison of antibacterial appearance among nanocomposites.

| Bacteria under Study | Catalyst used | Amount of catalyst | Inactivation efficiency | Refs. |
|---|---|---|---|---|
| *Escherichia coli* | nZVI | 7–700 mg | 25–90% | [40] |
| *Bacillus subtilis* | nZVI | 100–1000 mg | 80–100% | [14] |
| *Bacillus subtilis* | nZVI | 1000 mg | <90% | [41] |
| *E. coli* | nZVI | 1000 mg | ~100% | |
| *E. coli* | FeAg | 270 mg | More than 90% | [23] |
| *Bacillus subtilis* | GFeAg | 1–5 mg | More than 90% | This study |
| *E. coli* | GFeAg | 100 mg | More than 90% | |
| *Staphylococcus aureus* | GFeAg | 100 mg | More than 90% | |

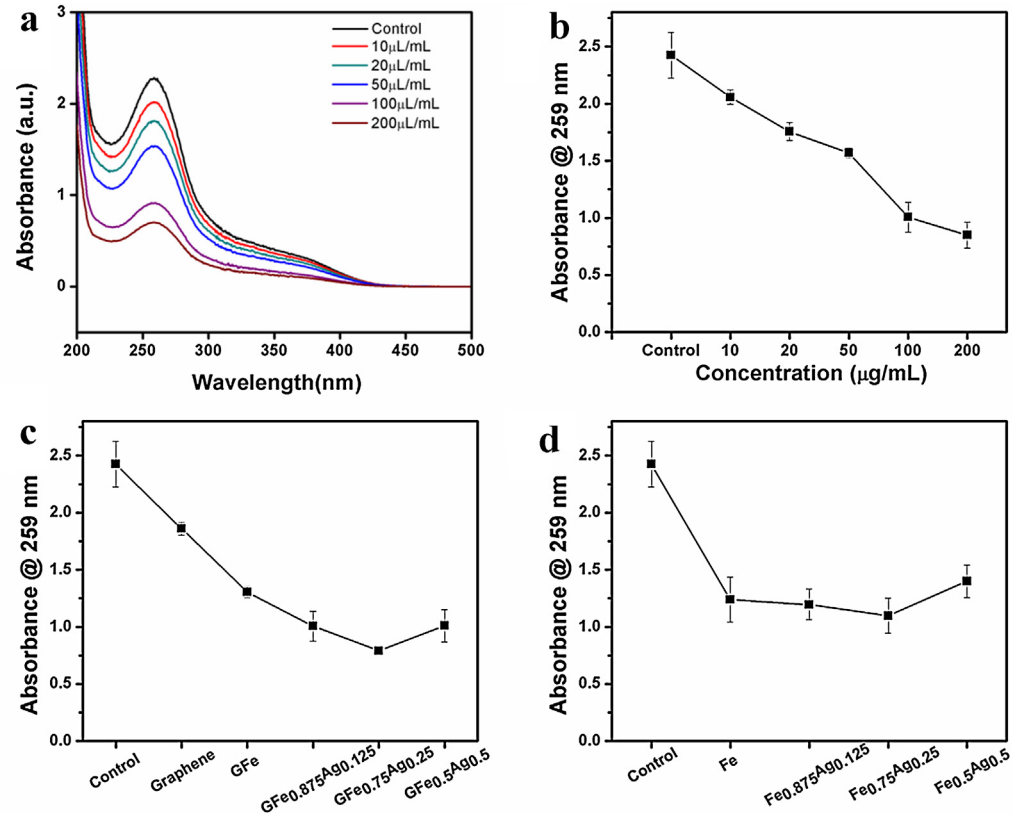


**Fig. 7.** (a) UV–vis spectra of ROS production during the incubation of $NBT^{2+}$ (0.2 mM) with different concentration of G-$Fe_7Ag_1$ (10–200 μg/mL). (b) The concentration dependence of ROS production in the presence of G-$Fe_7Ag_1$ (10–200 μg/mL). (c) $NBT^{2+}$ degradation by using different compositions of grapheme loaded metals (100 μg/mL), and (d) $NBT^{2+}$ degradation by using different compositions of metals without graphene support (100 μg/mL). Control means that there is no catalyst in the $NBT^{2+}$ solution.

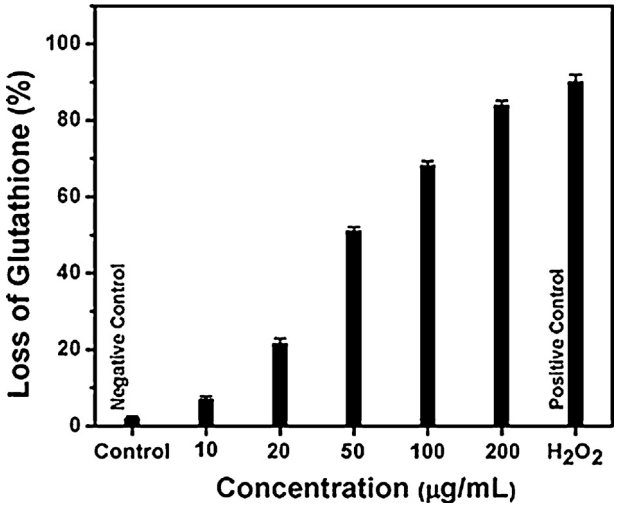


**Fig. 8.** Oxidation of glutathione (GSH) (0.4 mM) after *in vitro* incubation with different concentrations of $GFe_7Ag_1$, GSH without the addition of $GFe_7Ag_1$ was used as a negative control while 1 mM $H_2O_2$ is positive control.

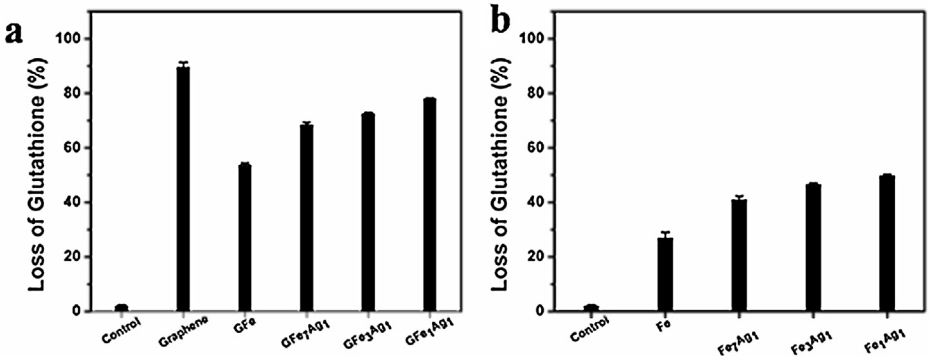


**Fig. 9.** Oxidation of glutathione by graphene and FeAg bimetallic nanocomposite (a) Graphene and different composition of graphene-FeAg dependent oxidation of GSH, (b) Effect of different bimetallic composition without graphene on the oxidation of GSH, (control means GSH solution without any nanocomposite).

The incubation condition in our experiment does not cause the oxidation of GSH as suggested by the negative control experiment. It is hypothesized that the GSH oxidation should be concentration dependent since the above antibacterial activity experiments indicate that cell viability is concentration dependent (Fig. 4). Therefore, oxidation of GSH was carried out under different concentrations of $GFe_7Ag_1$. Fig. 8 shows that the oxidation of GSH is increased from $7 \pm 0.8\%$ at 10 mg/L to $84 \pm 0.27\%$ at 200 μg/L concentration as the concentration of nanocomposite is enhanced. Such result is consistent to the concentration dependent increase in the antibacterial activity.

As presented in Fig. 9a, a noticeable fraction of GSH oxidation is observed when graphene and different compositions of graphene-bimetallic nanocomposites were used. Graphene shows much more oxidation as compared to other nanocomposites. The higher GSH oxidation of graphene might be attributed to its excellent electrical conductivity. In contrast to GSH oxidation of graphene, graphene presents less antibacterial activity. Antibacterial activity depends on size and despersibility. Similar observations were concluded with GSH oxidation using single wall carbon nanotubes and reduce graphene oxide [30,43]. Other graphene-bimetallic nanocomposites manifest slight variation for the oxidation of GSH.

To better understand the role of bimetallic and graphene in the oxidation of GSH, the effects of different composition of FeAg bimetallic graphene were also investigated. These results reveal that the loss of oxidation is decreased by using bimetallic without graphene. In the case of graphene based nanocomposite, graphene plays some role. For example, 100 μg/mL of $Fe_7Ag_1$ shows $41.05 \pm 1.2\%$ GSH oxidation while same composition of bimetallic with graphene shows $68.3 \pm 0.29\%$ GSH oxidation. These GSH oxidation results confirm that graphene based nanocomposites are better capable of arbitrating oxidative stress towards the bacterial cells through a ROS-independent way.

## 4. Proposed antibacterial mechanism

From the ROS and non ROS studies, it can be concluded that above mentioned possible ways might contribute together for antibacterial activity by bimetallic graphene nanocomposites.

Firstly, it can be concluded from the ROS study that ROS plays a role in the bacterial toxicity. ROS generated by graphene loaded nanocomposite is higher than FeAg bimetallic without graphene. Although FeAg bimetallic NPs without graphene also produce ROS but from the antibacterial data, it seems that ROS play its role up to some extent. Study reveals that ions in excess cause cell damages. In fact, ions of iron and silver essentially play the critical role in the antibacterial activity. Recent study elucidated the role of ions in the cell death in which ions and their derivatives play an important role for the functionality of ROS producing enzymes within

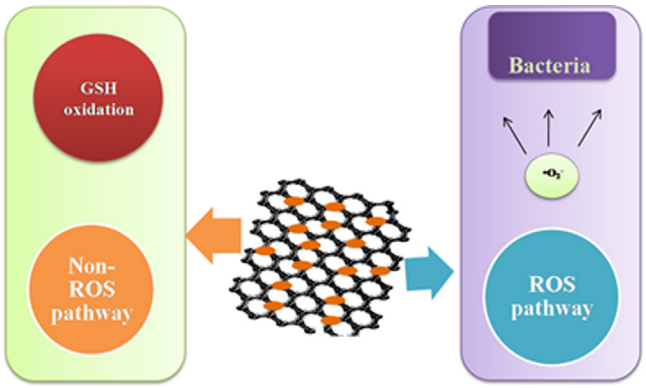


**Fig. 10.** Proposed antibacterial mechanism for the graphene loadeed FeAg nanocomposite.

the cells [47]. Excess of metal ions are capable of producing strong radicals *via* Fenton reaction with the $H_2O_2$ which are produced by superoxide dismutase reacting with the $^{\bullet}O_2^-$ according to following mechanism [48]. Despite the intracellular and extracellular ROS generation, some studies suggest that silver ions inhibits quinone oxidoreductase (NQR), a component of the respiratory chain of some bacteria, and causes the proton leakage [49].

Secondly, GSH oxidation or non-ROS path confirms its role in the death of bacterial cells. Our results show that antibacterial activity of graphene anchored FeAg nanocomposite is much higher as compare to the FeAg bimetallic itself. The oxidation of GSH further confirms these results. Graphene not only participates partially in the antibacterial activity but also provides a support for the bimetallic NPs. Bimetallic NPs is less efficient likely due to the aggregation of NPs and the oxidation of iron in aqueous solution since the particle size play a vital role in the toxicity of bacteria reported previously [30]. Graphene loaded FeAg nanocomposite shows better bacticidal activity because of smaller size of bimetallic NPs anchored on graphene as indicated in TEM images.

Finally, the effect from physical contact of material should not be excluded as the cause of the death of bacterial cells as reported in the previous studies [30]. Researchers claimed that cells would be trapped in the graphene sheets or biological membrane consisting of amphiphilic phospholipids molecules would trap the small graphene sheet [50].

From above mentioned results and previous studies, there could be different possible mechanisms (Fig. 10) involved in the antibacterial activity by the graphene loaded FeAg nanocomposite including membrane disruptive interaction, bacteria-nanocomposite interaction, and oxidizing the cellular components as discussed in the previous studies [30,42]. ROS generation outside the cells and

within the cells play some role in the toxicity towards bacteria, while the release of metal ions from the nanocomposite may react with $^{\bullet}O_2^-$ to produce the strong $^{\bullet}OH$ radicals. The strong oxidation of GSH by the nanocomposite suggests that they also play major role for the antibacterial activity. Bacterial death might occur because nanocomposite directly contact with the bacteria due to its smaller size and surface area in the current case. Graphene itself may also play some role in the membrane stress due to its sharp edges [30].

## 5. Conclusion

Bimetallic FeAg with different composition of iron and silver were synthesized on graphene in one step. The characterizations by TEM, XRD, EDS, and Raman reveal that these nanocomposites are fabricated successfully. The antibacterial activities of these nanocomposites were evaluated by using three different bacteria (*B. subtilis, E. coli, and S. aureus*). The nanocomposites demonstrate excellent antibacterial activity as compared to bare FeAg bimetallic. The effective antibacterial capability of these nanocomposites is largely due to well dispersed FeAg bimetallic on the promising graphene support. The antibacterial activity of graphene loaded nanocomposite may be endorsed due to the membrane and oxidative stress. The possible antibacterial mechanism may be studied by reactive oxygen species (ROS) and GSH oxidation (Non-ROS). Results from NBT degradation show that ROS are produced in the system which might cause the cell death. Despite these ROS results, GSH oxidation suggests that these nanocomposites are able to put non-ROS oxidative stress on the bacterial cell. From these results, we may conclude that antibacterial activity of graphene loaded FeAg is mainly due to the non-ROS oxidative stress while ROS plays a minor role.

## Acknowledgements

We acknowledge the financial support from the National Natural Science Foundation of China (Nos. 51273063, 21476143, and 21306049), the Fundamental Research Funds for the Central Universities, the higher school specialized research fund for the doctoral program (222201313005 and 222201314029), 111 Project Grant (B08021), the Open Project of State Key Laboratory of Chemical Engineering (SKL-ChE-14C01), and Innovation Program of Shanghai Municipal Education Commission (15ZZ030).

## Appendix A. Supplementary data

Supplementary data associated with this article can be found, in the online version, at http://dx.doi.org/10.1016/j.colsurfb.2016.03.065.

## References

[1] M.-F. Hou, L. Liao, W.-D. Zhang, X.-Y. Tang, H.-F. Wan, G.-C. Yin, Degradation of rhodamine B by Fe(0)-based fenton process with $H_2O_2$, Chemosphere 83 (2011) 1279–1283.
[2] R.A. Crane, T.B. Scott, Nanoscale zero-valent iron: future prospects for an emerging water treatment technology, J. Hazard. Mater. 211–212 (2012) 112–125.
[3] Y. Huang, H. Ma, S. Wang, M. Shen, R. Guo, X. Cao, M. Zhu, X. Shi, Efficient catalytic reduction of hexavalent chromium using palladium nanoparticle-immobilized electrospun polymer nanofibers, ACS Appl. Mater. Interfaces 4 (2012) 3054–3061.
[4] J. Mansfield, S. Genin, S. Magori, V. Citovsky, M. Sriariyanum, P. Ronald, M. Dow, V. Verdier, S.V. Beer, M.A. Machado, Top 10 plant pathogenic bacteria in molecular plant pathology, Mol. Plant Pathol. 13 (2012) 614–629.
[5] K. Turcheniuk, C.-H. Hage, J. Spadavecchia, A.Y. Serrano, I. Larroulet, A. Pesquera, A. Zurutuza, M.G. Pisfil, L. Héliot, J. Boukaert, Plasmonic photothermal destruction of uropathogenic *E. coli* with reduced graphene oxide and core/shell nanocomposites of gold nanorods/reduced graphene oxide, J. Mater. Chem. B 3 (2015) 375–386.
[6] D. Lebeaux, A. Chauhan, O. Rendueles, C. Beloin, From in vitro to in vivo models of bacterial biofilm-related infections, Pathogens 2 (2013) 288–356.
[7] A.F. de Faria, D.S.T. Martinez, S.M.M. Meira, A.C.M. de Moraes, A. Brandelli, A.G. Souza Filho, O.L. Alves, Anti-adhesion and antibacterial activity of silver nanoparticles supported on graphene oxide sheets, Colloids Surf. B 113 (2014) 115–124.
[8] I. Sondi, B. Salopek-Sondi, Silver nanoparticles as antimicrobial agent: a case study on *E. coli* as a model for gram-negative bacteria, J. Colloids Interf. Sci. 275 (2004) 177–182.
[9] S.J. Lee, D.N. Heo, J.-H. Moon, W.-K. Ko, J.B. Lee, M.S. Bae, S.W. Park, J.E. Kim, D.H. Lee, E.-C. Kim, C.H. Lee, I.K. Kwon, Electrospun chitosan nanofibers with controlled levels of silver nanoparticles. Preparation, characterization and antibacterial activity, Carbohydr. Polym. 111 (2014) 530–537.
[10] P.A. Frey, G.H. Reed, The ubiquity of iron, ACS Chem. Biol. 7 (2012) 1477–1481.
[11] H. Kim, H.-J. Hong, J. Jung, S.-H. Kim, J.-W. Yang, Degradation of trichloroethylene (TCE) by nanoscale zero-valent iron (nZVI) immobilized in alginate bead, J. Hazard. Mater. 176 (2010) 1038–1043.
[12] R. Li, X. Jin, M. Megharaj, R. Naidu, Z. Chen, Heterogeneous Fenton oxidation of 2,4-dichlorophenol using iron-based nanoparticles and persulfate system, Chem. Eng. J. 264 (2015) 587–594.
[13] C. Üzüm, T. Shahwan, A.E. Eroğlu, I. Lieberwirth, T.B. Scott, K.R. Hallam, Application of zero-valent iron nanoparticles for the removal of aqueous $Co^{2+}$ ions under various experimental conditions, Chem. Eng. J. 144 (2008) 213–220.
[14] M. Diao, M. Yao, Use of zero-valent iron nanoparticles in inactivating microbes, Water Res. 43 (2009) 5243–5251.
[15] Q. Chen, M. Gao, J. Li, F. Shen, Y. Wu, Z. Xu, M. Yao, Inactivation and magnetic separation of bacteria from liquid suspensions using electrosprayed and nonelectrosprayed nZVI particles: observations and mechanisms, Environ. Sci. Technol. 46 (2012) 2360–2367.
[16] Z. Li, K. Greden, P.J.J. Alvarez, K.B. Gregory, G.V. Lowry, Adsorbed polymer and NOM limits adhesion and toxicity of nano scale zerovalent iron to *E. coli*, Environ. Sci. Technol. 44 (2010) 3462–3467.
[17] C. Lee, J.Y. Kim, W.I. Lee, K.L. Nelson, J. Yoon, D.L. Sedlak, Bactericidal effect of zero-valent iron nanoparticles on *Escherichia coli*, Environ. Sci. Technol. 42 (2008) 4927–4933.
[18] K.J. Carroll, D.M. Hudgins, S. Spurgeon, K.M. Kemner, B. Mishra, M.I. Boyanov, L.W. Brown III, M.L. Taheri, E.E. Carpenter, One-pot aqueous synthesis of Fe and Ag core/shell nanoparticles, Chem. Mater. 22 (2010) 6291–6296.
[19] N.F. Adegboyega, V.K. Sharma, K.M. Siskova, R. Vecerova, M. Kolar, R. Zbořil, J.L. Gardea-Torresdey, Enhanced formation of silver nanoparticles in $Ag^+$-NOM-Iron(II, III) systems and antibacterial activity studies, Environ. Sci. Technol. 48 (2014) 3228–3235.
[20] K.J.P. Anthony, M. Murugan, S. Gurunathan, Biosynthesis of silver nanoparticles from the culture supernatant of *Bacillus marisflavi* and their potential antibacterial activity, J. Ind. Eng. Chem. 20 (2014) 1505–1510.
[21] Y.-S. Ko, Y.H. Joe, M. Seo, K. Lim, J. Hwang, K. Woo, Prompt and synergistic antibacterial activity of silver nanoparticle-decorated silica hybrid particles on air filtration, J. Mater. Chem. B 2 (2014) 6714–6722.
[22] Z.-m. Xiu, Q.-b. Zhang, H.L. Puppala, V.L. Colvin, P.J.J. Alvarez, Negligible particle-specific antibacterial activity of silver nanoparticles, Nano Lett. 12 (2012) 4271–4275.
[23] Z. Markovaí, K.M. n. Šiškovaí, J. Filip, J. Čuda, M. Kolaíř, K. r. Šafaířovaí, I. Medřiík, R. Zbořil, Air stable magnetic bimetallic Fe–Ag nanoparticles for advanced antimicrobial treatment and phosphorus removal, Environ. Sci. Technol. 47 (2013) 5285–5293.
[24] K.S. Novoselov, V.I. Falko, L. Colombo, P.R. Gellert, M.G. Schwab, K. Kim, A roadmap for graphene, Nature 490 (2012) 192–200.
[25] B. Paul, V. Parashar, A. Mishra, Graphene in the $Fe_3O_4$ nano-composite switching the negative influence of humic acid coating into an enhancing effect in the removal of arsenic from water, Environ. Sci.: Water Res. Technol. 1 (2015) 77–83.
[26] A. Kumar, S. Husale, A.K. Srivastava, P.K. Dutta, A. Dhar, Cu-Ni nanoparticle-decorated graphene based photodetector, Nanoscale 6 (2014) 8192–8198.
[27] H. Jabeen, V. Chandra, S. Jung, J.W. Lee, K.S. Kim, S.B. Kim, Enhanced Cr(vi) removal using iron nanoparticle decorated graphene, Nanoscale 3 (2011) 3583–3585.
[28] O. Akhavan, E. Ghaderi, Photocatalytic reduction of graphene oxide nanosheets on $TiO_2$ thin film for photoinactivation of bacteria in solar light irradiation, J. Phys. Chem. C 113 (2009) 20214–20220.
[29] T. Tian, X. Shi, L. Cheng, Y. Luo, Z. Dong, H. Gong, L. Xu, Z. Zhong, R. Peng, Z. Liu, Graphene-based nanocomposite as an effective, multifunctional, and recyclable antibacterial agent, ACS Appl. Mater. Interfaces 6 (2014) 8542–8548.
[30] S. Liu, T.H. Zeng, M. Hofmann, E. Burcombe, J. Wei, R. Jiang, J. Kong, Y. Chen, Antibacterial activity of graphite, graphite oxide, graphene oxide, and reduced graphene oxide: membrane and oxidative stress, ACS Nano 5 (2011) 6971–6980.
[31] W. Hu, C. Peng, W. Luo, M. Lv, X. Li, D. Li, Q. Huang, C. Fan, Graphene-based antibacterial paper, ACS Nano 4 (2010) 4317–4323.
[32] W.S. Hummers, R.E. Offeman, Preparation of graphitic oxide, J. Am. Chem. Soc. 80 (1958), 1339–1339.
[33] P. Cheng, Z. Yang, H. Wang, W. Cheng, M. Chen, W. Shangguan, G. Ding, $TiO_2$–graphene nanocomposites for photocatalytic hydrogen production from splitting water, Int. J. Hydrogen Energy 37 (2012) 2224–2230.

[34] C. Zhao, L.E. Arroyo-Mora, A.P. DeCaprio, V.K. Sharma, D.D. Dionysiou, K.E. O'Shea, Reductive and oxidative degradation of iopamidol iodinated X-ray contrast media, by Fe(III)-oxalate under UV and visible light treatment, Water Res. 67 (2014) 144–153.
[35] X. Yang, C. Chen, J. Li, G. Zhao, X. Ren, X. Wang, Graphene oxide-iron oxide and reduced graphene oxide-iron oxide hybrid materials for the removal of organic and inorganic pollutants, RSC Adv. 2 (2012) 8821–8826.
[36] L. Zheng, G. Zhang, M. Zhang, S. Guo, Z.H. Liu, Preparation and capacitance performance of Ag–graphene based nanocomposite, J. Power Sources 201 (2012) 376–381.
[37] F. Ren, C. Wang, C. Zhai, F. Jiang, R. Yue, Y. Du, P. Yang, J. Xu, One-pot synthesis of a RGO-supported ultrafine ternary PtAuRu catalyst with high electrocatalytic activity towards methanol oxidation in alkaline medium, J. Mater. Chem. A 1 (2013) 7255–7261.
[38] M. Zhu, Y. Dong, B. Xiao, Y. Du, P. Yang, X. Wang, Enhanced photocatalytic hydrogen evolution performance based on Ru-trisdicarboxybipyridine-reduced graphene oxide hybrid, J. Mater. Chem. 22 (2012) 23773–23779.
[39] A. Ahmad, X. Gu, L. Li, S. Lv, Y. Xu, X. Guo, Efficient degradation of trichloroethylene in water using persulfate activated by reduced graphene oxide-iron nanocomposite, Environ. Sci. Pollut. Res. 22 (2015) 17876–17885.
[40] M. Auffan, W. Achouak, J. Rose, M.-A. Roncato, C. Chanéac, D.T. Waite, A. Masion, J.C. Woicik, M.R. Wiesner, J.-Y. Bottero, Relation between the redox state of iron-based nanoparticles and their cytotoxicity toward *Escherichia coli*, Environ. Sci. Technol. 42 (2008) 6730–6735.
[41] J. Chen, Z. Xiu, G.V. Lowry, P.J.J. Alvarez, Effect of natural organic matter on toxicity and reactivity of nano-scale zero-valent iron, Water Res. 45 (2011) 1995–2001.
[42] X. Yang, J. Li, T. Liang, C. Ma, Y. Zhang, H. Chen, N. Hanagata, H. Su, M. Xu, Antibacterial activity of two-dimensional $MoS_2$ sheets, Nanoscale 6 (2014) 10126–10133.
[43] C.D. Vecitis, K.R. Zodrow, S. Kang, M. Elimelech, Electronic-structure-dependent bacterial cytotoxicity of single-walled carbon nanotubes, ACS Nano 4 (2010) 5471–5479.
[44] Z. Xiong, B. Lai, P. Yang, Y. Zhou, J. Wang, S. Fang, Comparative study on the reactivity of Fe/Cu bimetallic particles and zero valent iron (ZVI) under different conditions of $N_2$, air or without aeration, J. Hazard. Mater. 297 (2015) 261–268.
[45] C.-H. Deng, J.-L. Gong, G.-M. Zeng, C.-G. Niu, Q.-Y. Niu, W. Zhang, H.-Y. Liu, Inactivation performance and mechanism of *Escherichia coli* in aqueous system exposed to iron oxide loaded graphene nanocomposites, J. Hazard. Mater. 276 (2014) 66–76.
[46] G.L. Ellman, Tissue sulfhydryl groups, Arch. Biochem. Biophys. 82 (1959) 70–77.
[47] S.J. Dixon, B.R. Stockwell, The role of iron and reactive oxygen species in cell death, Nat. Chem. Biol. 10 (2014) 9–17.
[48] N.D. Vaziri, Understanding iron: promoting its safe use in patients with chronic kidney failure treated by hemodialysis, Am. J. Kidney Dis. 61 (2013) 992–1000.
[49] J.A. Lemire, J.J. Harrison, R.J. Turner, Antimicrobial activity of metals: mechanisms, molecular targets and applications, Nat. Rev. Microbiol. 11 (2013) 371–384.
[50] A.V. Titov, P. Král, R. Pearson, Sandwiched graphene-membrane superstructures, ACS Nano 4 (2010) 229–234.